Using the first of the above expressions for AN, it follows that

$$a = \frac{BB'}{AN} = \frac{l_1}{l_0 \sin \chi_0} \cdot \frac{\sin (\lambda_0 - \lambda_1)}{\sin \lambda_0}.$$

In order to simplify the formulæ we denote $\frac{l_1}{l_0} = 1 + \delta$ by d, and after eliminating λ_1, we finally obtain, with the aid of the extension formula (26/1)

$$a = \frac{1}{\sin \chi_0} (\sqrt{d^2 - \sin^2 \lambda_0} - \cos \lambda_0) \quad . \quad . \quad (26/3)$$

In this formula the glide strain is expressed by the *initial position*

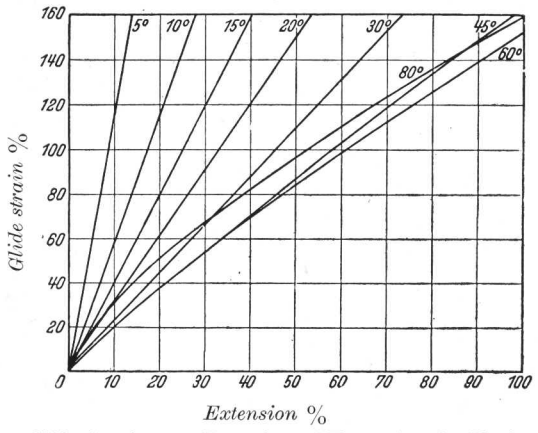

FIG. 37.—Glide Strain as a Function of Extension for Various Initial Angles of the Glide Plane.

of the glide elements and by the amount of extension. If, instead of the extension, the final position of the glide elements is introduced, the following formulæ, which are particularly convenient for numerical calculations, are obtained :

$$a = \frac{\cos \lambda}{\sin \chi} - \frac{\cos \lambda_0}{\sin \chi_0} \quad . \quad . \quad . \quad . \quad . \quad (26/4)$$

or

$$a = (\cot \lambda - \cot \lambda_0) \frac{\sin \lambda_0}{\sin \chi_0} \quad . \quad . \quad . \quad (26/4a)$$

The formula (26/3) shows that equal extensions may be accompanied by different amounts of glide strain, dependent upon the initial position of the glide elements. How strong the effect of the orientation is, can be seen from Fig. 37, in which the glide strain is

expressed as a function of the extension for various initial angles of the glide plane (for the sake of simplicity $\lambda_0 = \chi_0$ has been chosen). For *every* position of the glide elements the glide strain corresponding to a small extension can be calculated according to the formula

$$\Delta a = \frac{\Delta d}{\sin \chi_0 \cos \lambda}$$

which is obtained by differentiation from the equation (26/3).

Another formal description of glide (by means of a transformation of co-ordinates) which we shall use in what follows, is contained in Fig. 38. The xy plane represents the glide plane and the y axis the glide direction. Let OP_0 be the length of the crystal to be stretched; the direction of tension is given with reference to the glide elements by the co-ordinates $(x_0y_0z_0)$. When glide occurs there is a gliding parallel to T in the direction t, as a result of which P_0 arrives at P_1. Let a represent the crystallographic glide strain, the glide displacement is then given by the product $a \,.\, z_0$. Hence, the transformation of the co-ordinates is:

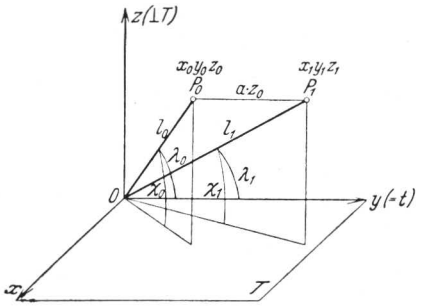

FIG. 38.—Diagram to Illustrate Glide by Means of a Transformation of Co-ordinates.

$$\begin{aligned} x_1 &= x_0 \\ y_1 &= y_0 + z_0 \,.\, a \\ z_1 &= z_0 \end{aligned}$$

and for

$$\frac{l_1}{l_0} = \sqrt{\frac{x_1^2 + y_1^2 + z_1^2}{x_0^2 + y_0^2 + z_0^2}}$$

we obtain

$$\frac{l_0}{l_1} = \sqrt{1 + \frac{2ay_0z_0 + a^2z_0^2}{l_0^2}}.$$

Further, since $y_0 = l_0 \cos \lambda_0$ and $z_0 = l_0 \sin \chi_0$ we have

$$\frac{l_1}{l_0} = d = 1 + \delta = \sqrt{1 + 2a \sin \chi_0 \cos \lambda_0 + a^2 \sin^2 \chi_0} \quad . \quad (26/5)$$

In this formula the extension is expressed by the glide strain and

the initial orientation of the glide elements; it is also obtained directly by solving, *e.g.*, (26/3), with respect to d.

By means of this representation of glide it is now quite easy to follow the change of the cross-section which occurs during extension of cylindrical crystals. It has already been pointed out that the elliptical cylinder (the ribbon), which develops during glide, is usually broader than the original crystal. In what follows, the expressions for the two semi-axes of the elliptic cross-section will be given as functions of the original orientation and the orientation at any given moment in the course of extension (99). These formulæ are obtained as follows :

We start by finding the equation of the original cylinder in the co-ordinate system shown in Fig. 38. By introducing the transformed co-ordinates which correspond to the glide we obtain the equation of an elliptical cylinder, which is compared with the normal form. In this way the following expression is obtained :

$$2 + a^2 \sin^2 \lambda_0 + 2a \sin \chi_0 \cos \lambda_0 = R^2 \cdot \left(\frac{1}{A^2} + \frac{1}{B^2}\right),$$

in which R denotes the radius of the initial circular section, A and B the half-axes of the sectional ellipse after extension. If now we bear in mind that the volume remains constant during extension by glide [1] ($R^2\pi l_0 = AB\pi l_1$) it follows that after some calculation

$$p^4 - p^2\left(\frac{2 \cos (\lambda_0 - \lambda) \cdot \sin \lambda}{\sin \lambda_0} + \frac{\sin^2 (\lambda_0 - \lambda)}{\sin^2 \chi_0}\right) + \frac{\sin^2 \lambda}{\sin^2 \lambda_0} = 0 \quad . \quad (26/6)$$

The four roots p_i of this equation, of which two each differ only by the sign, are the desired ratios $\frac{A}{R}$ and $\frac{B}{R}$.

Two special cases must be briefly mentioned. For $\lambda_0 = \chi_0$, *i.e.*, for glide along the great axis of the translation ellipses, there are two roots of the equation equal to 1. The width of the band always coincides with the diameter of the initial section. The second special case relates to the maximum width at infinite extension (94). This case corresponds to the convergence of the longitudinal direction towards the operative glide direction. $\lambda = 0$ must therefore be inserted in the above formula, and the limiting value for increase in width by simple glide is then found to be

$$\left(\frac{A}{R}\right)_{\text{max.}} = \frac{\sin \lambda_0}{\sin \chi_0} \quad . \quad . \quad . \quad . \quad (26/6a)$$

[1] How exactly this condition is fulfilled will be shown in Section 60.

If for λ_0 we substitute the angle κ_0 between the direction of glide and the great axis of the glide ellipses, the maximum increase in width can also be expressed by the formula

$$\left(\frac{A}{R}\right)_{\max} = \sqrt{\frac{\sin^2 \kappa_0}{\sin^2 \chi_0} + \cos^2 \kappa_0} \quad . \quad . \quad (26/6b)$$

since χ_0, λ_0 and κ_0 are connected by the relationship $\cos \lambda_0 = \cos \chi_0 \cdot \cos \kappa_0$ (cf. Fig. 39).

Simple glide in *compression* can be described much more briefly [(100), (101)]. Fig. 40 shows diagrammatically a crystal specimen before and after compression. Contrary to expectation the lattice rotation which accompanies compression is not simply the opposite of that which occurs in tension.

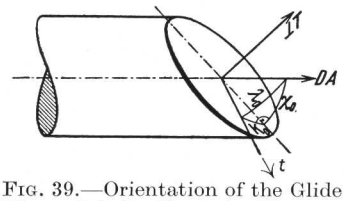

FIG. 39.—Orientation of the Glide Elements in the Crystal. Diagram Illustrating an Analysis of the Components of Tensile Stress.

If, in the compression test, the longitudinal direction is regarded as that of the normal to the compression plates, then on the great circle this will not move away from the operative glide direction. Lattice rotation takes the form rather of an approach of the longitudinal direction to the pole of the

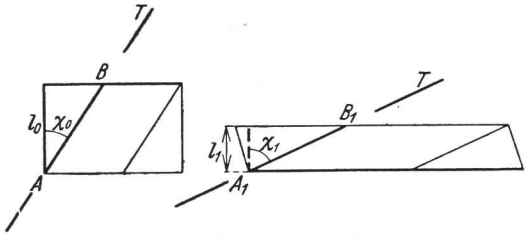

FIG. 40.—Diagram Illustrating Glide in Compression.

glide plane, which follows directly from the fact that the line of intersection of the glide plane with the compression plates retains the same inclination to the crystal axes throughout the test.

The formula connecting compression with glide strain can also be found directly from Fig. 40. Let χ_0 and χ_1 be again the angles between the glide plane and the longitudinal direction before and after compression; then

$$e = \left(\frac{l_1}{l_0}\right) = \frac{\cos \chi_1}{\cos \chi_0} \quad . \quad . \quad . \quad . \quad . \quad (26/7)$$

and since the eccentricity (κ) of the glide direction, corresponding to the rotation of the lattice, remains constant, this formula can be extended to include also λ_0 and λ_1.

The relationship between glide strain and compression is then

$$\frac{1}{e^2} = \left(\frac{l_0}{l_1}\right)^2 = 1 + 2a \sin \chi_0 \cos \lambda_0 + a^2 \cos^2 \lambda_0 \quad . \quad (26/8)$$

In the case of plastic *bending* by glide, the exact geometrical treatment of which has still to be formulated, parallel epipedic plates acquire as a rule a saddle shape [aluminium crystals (102)]. When the operative glide elements are in a certain special position relative to the axis of bending, cylindrical bending can also occur.

27. *Transformation of Indices in Glide*

In Section 26 we discussed the relation of glide to lattice rotation and deformation. In the present section we will deal briefly with its effect on the crystallographic symbols of directions and planes. From the rotation during glide of the longitudinal axis of the specimen relative to the crystallographic axes, it is apparent that the indices are not retained. In general, the atomic array constituting a direction or a plane changes its crystallographic nature continuously during glide.

Let (HKL) be the indices of the glide plane, $[UVW]$ those of the glide direction, then the following transformation formulæ will apply according to (103) :

The direction $[uvw]$ is transformed into $[u'v'w']$ by

$$\left.\begin{aligned} u' &= u + U(uH + vK + wL)N \\ v' &= v + V(uH + vK + wL)N \\ w' &= w + W(uH + vK + wL)N \end{aligned}\right\} \quad . \quad . \quad . \quad . \quad (27/1)$$

The plane (hkl) is transformed into $(h'k'l')$ by

$$\left.\begin{aligned} h' &= h + V(hK - kH)N + W(hL - lH)N \\ k' &= k + U(kH - hK)N + W(kL - lK)N \\ l' &= l + U(lH - hL)N + V(lK - kL)N \end{aligned}\right\} \quad . \quad (27/2)$$

in which N is a whole number and signifies the number of interatomic distances by which two neighbouring glide planes are displaced relative to one another.

The directions and planes for which the indices are retained during glide can be readily recognized from these equations. The glide plane is the geometrical location of all directions which remain

invariable relative to glide, the zone of the glide direction contains all planes whose symbol remains unchanged during glide.

28. *Double Glide*

Owing to the symmetry of crystals, the plane and direction of glide are not usually unique elements of the lattice. It may often happen, therefore, that two or more crystallographically equivalent glide systems will be equivalent geometrically, and so become operative in plastic deformation. So far only the simultaneous activity of two crystallographically equivalent systems has been considered in detail.

The simplest case is that of glide in two directions in the same plane. Double glide in this instance is gliding on the same plane, with the bisector of the angle of the two glide directions serving as direction of glide. The lattice rotation which accompanies extension consists in a movement of the longitudinal direction towards the line of symmetry of the two glide directions. The only extension formula to remain valid is (26/2), with which (26/1) conforms, provided that the angles formed with the " resulting glide direction " are now designated λ.

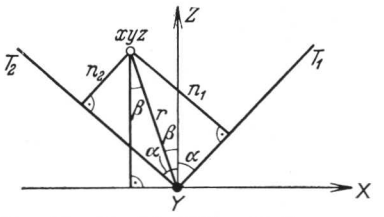

FIG. 41.—Double Glide with Common Direction of Glide.

The next case concerns the simultaneous operation of two glide planes with a common glide direction (their line of intersection). In the diagram shown in Fig. 41 the common glide direction coincides with the y-axis (which is perpendicular to the plane of the drawing) of the system of co-ordinates that is symmetrical to the two glide systems. The resulting displacement (Δy) of a point P is composed of the two separate displacements. Let a again represent the glide strain which is equal for the two systems; the glide displacements are then given by the products an_1 and an_2; and $\Delta y = an_1 + an_2$ represents the total glide strain. If now the two expressions which follow directly from Fig. 41 :

$$n_1 = r \sin (\alpha + \beta)$$
$$n_2 = r \sin (\alpha - \beta)$$

are inserted for n_1 and n_2, we obtain finally

$$\Delta y = 2a \sin \alpha \, . \, z,$$

i.e., the resulting movement is equivalent to a simple glide along the x–y plane in the common glide direction, that of the y-axis.

The yz-plane, too, contains the common glide direction and lies symmetrically to the two planes T_1 and T_2. Which of these two planes of symmetry is to be regarded as the resultant glide plane depends upon the direction of the imposed deformation. Deformation is accompanied by lattice rotation in the same way as in *simple* glide; the extension formula (26/1), relating to the common glide direction applies.

The third case to be discussed arises when neither glide plane nor glide direction is common to the two glide systems (Fig. 42). In order to superpose the two glides in the case of an extension [(104), (105)] we represent glide by means of a co-ordinate transformation (106) which was given in Section 26. We transform the glides which occur in the systems xyz and $x'y'z'$ to a new rectangular

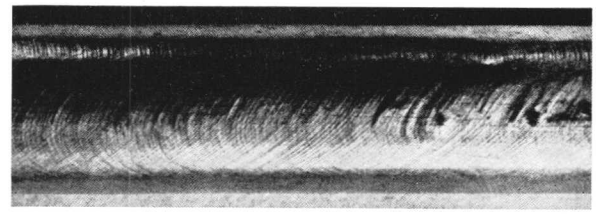

FIG. 42.—α-Brass Crystal Showing Double Glide (103a).

system $\xi\eta\zeta$. The position of the new axes in relation to the old ones is given by the two matrices of the direction cosines :

	x	y	z
ξ	a_1	b_1	c_1
η	a_2	b_2	c_2
ζ	a_3	b_3	c_3

and

	x'	y'	z'
ξ	a'_1	b'_1	c'_1
η	a'_2	b'_2	c'_2
ζ	a'_3	b'_3	c'_3

The changes in the co-ordinates due to glide were, in view of the special position of the co-ordinate system,

$$\begin{cases} \Delta x = 0 \\ \Delta y = az_0 \\ \Delta z = 0 \end{cases} \quad \text{and} \quad \begin{cases} \Delta x' = 0 \\ \Delta y' = a'z_0 \\ \Delta z' = 0 \end{cases}$$

These have now to be transformed into the new common system of co-ordinates $\xi\eta\zeta$. The changes $\Delta\xi$, $\Delta\eta$, $\Delta\zeta$ amount to :

$$\begin{cases} \Delta\xi = a_1\Delta x + b_1\Delta y + c_1\Delta z + a'_1\Delta x' + b'_1\Delta y' + c'_1\Delta z' \\ \Delta\eta = a_2\Delta x + \ldots \qquad\qquad + a'_2\Delta x' + \ldots \\ \Delta\zeta = a_3\Delta x + \ldots \qquad\qquad + a'_3\Delta x' + \ldots \end{cases}$$

Since Δx, $\Delta x'$, Δz, and $\Delta z' = 0$, the equations can be simplified to :

$$\begin{cases} \Delta\xi = b_1\Delta y + b'_1\Delta y' \\ \Delta\eta = b_2\Delta y + b'_2\Delta y' \\ \Delta\zeta = b_3\Delta y + b'_3\Delta y'. \end{cases}$$

The equations can be further simplified if the new system of co-ordinates is symmetrical to the two glide systems. Let the ζ-axis be perpendicular both to the z and z'-axes; it is then the line of intersection of the two glide planes (of the xy plane with the $x'y'$ plane). Let the $\eta\zeta$ plane bisect the angle between the two glide planes. The z-, z'-, η- and ξ-axes then lie in a plane perpendicular to ζ (Fig. 43). From these conditions there follow for the direction cosines the relationships :

$$\begin{array}{ll} c_3 = c'_3 = 0 & (\zeta \perp z,\ \zeta \perp z') \\ c_2 = c'_2 & (\sphericalangle \eta z = \sphericalangle \eta z') \\ c_1 = -\,c'_1 & (\sphericalangle \xi z = \sphericalangle \xi z') \end{array}$$

$b_1 = -\,b'_1$, $b_2 = b'_2$, $b_3 = b'_3$ (y-axes symmetrical to the η-ζ plane). In this way

$$\begin{cases} \Delta\xi = b_1(\Delta y - \Delta y') = b_1(az_0 - a'z'_0) \\ \Delta\eta = b_2(\Delta y + \Delta y') = b_2(az_0 + a'z'_0) \\ \Delta\zeta = b_3(\Delta y + \Delta y') = b_3(az_0 + a'z'_0). \end{cases}$$

Assuming that the glide strains in both systems are of the same magnitude ($a = a'$),

$$\begin{cases} \Delta\xi = ab_1(z_0 - z'_0) \\ \Delta\eta = ab_2(z_0 + z'_0) \\ \Delta\zeta = ab_3(z_0 + z'_0) \end{cases}$$

in which z_0 and z'_0 are still to be expressed by ξ, η, ζ. From the above equations ($c_3 = c'_3 = 0$) we obtain $z_0 = c_1\xi + c_2\eta$,

hence $$z'_0 = -\,c_1\xi + c_2\eta$$

so that for simultaneous glide of magnitude a on each of the systems we finally obtain the following formulæ :

$$\left.\begin{array}{ll} \Delta\xi = 2ab_1c_2 \,.\, \xi & . \ . \ . \ . \ . \\ \Delta\eta = 2ab_2c_2 \,.\, \eta & . \ . \ . \ . \ . \\ \Delta\zeta = 2ab_3c_2 \,.\, \eta & . \ . \ . \ . \ . \end{array}\right\} \quad (28/1)$$

If, when double glide begins, the axis of rotation is in the plane $\eta\zeta$, which is symmetrical to the two glide systems, then $\xi = 0$ and

$\Delta\xi = 0$. This means, however, that in the case of equal glide strain in both systems the wire axis will remain always in the $\eta\zeta$ plane.[1]

The resulting movement can now be described in the same way as for simple glide by introducing the resulting glide direction τ (Fig. 44), whose angle ψ to the η-axis is given by the expression

$$tg\,\psi = \frac{\Delta\zeta}{\Delta\eta} = \frac{b_3}{b_2}$$

If ε is the angle between the axis of the bar and the resultant glide direction τ then it follows from Fig. 44 :

$$\frac{l_1}{l_0} = \frac{\sin\varepsilon_0}{\sin\varepsilon_1} \quad . \quad . \quad . \quad . \quad . \quad (28/2)$$

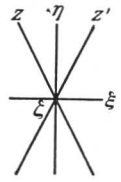

Fig. 43. Orientation of the New System of Co-ordinates in the Case of Double Glide.

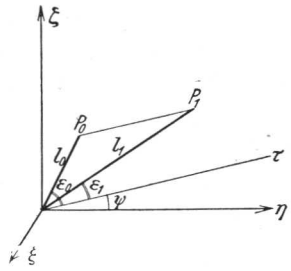

Fig. 44.—Double Glide in the New System of Co-ordinates.

From this extension formula for double glide it is again apparent that, so long as the wire axis remains in the same plane during rotation, the ensuing lattice rotation will follow the same law as applies to simple glide, with the resulting glide direction assuming the role of the glide direction. Just as the glide direction is attained by simple glide only after infinite extension, so, too, in double glide the resultant glide direction represents the final position of the wire axis for infinite extension. However, the purely formal nature of this analogy can be seen from the fact that a crystal whose longitudinal axis is parallel to the glide direction cannot be extended; on the other hand, if the longitudinal axis coincides with the resultant glide direction, it can be extensible by any amount by double glide, without change of orientation.

It is unnecessary to examine the formula by which glide strain

[1] But if the wire axis is not originally in the plane of symmetry, then it will move in a plane which is inclined towards it.

and extension are connected [cf. (99) and (107)]. For particulars of double glide in *compression*, readers are referred to the literature [(100), (101)].

29. *Formation of Spurious Glide Bands*

On the surface of extended crystals, in addition to the typical glide bands, other elliptical markings whose plane is usually inclined to the wire axis in a direction opposite to that of the glide bands (Fig. 45) are sometimes observed. That this second set of markings does not represent traces of crystallographic planes is shown by the fact that, in contrast to the glide ellipses, the eccentricity of these ellipses increases with increasing extension. A geometrical consideration of these markings reveals that they are obviously due to the distortion of grooves which originally ran circumferentially on the crystal (growth defects) (94).[1]

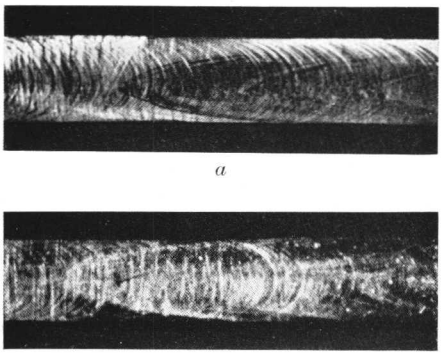

a

b

FIG. 45 (*a*) and (*b*).—Extended Zinc Crystals with Markings.

The special case of $\chi = \lambda$ ($\varkappa = 0$), which does not restrict the generality of the conclusions arrived at, is illustrated in Fig. 46. This shows the plane through the longitudinal axis of the crystal (l_0 or l_1), and the slip direction (AB). The plane BC of the groove which ran originally perpendicularly to the longitudinal direction arrives by glide in the position BC_1, which makes the angle ω_1 with the longitudinal axis of the extended crystal.

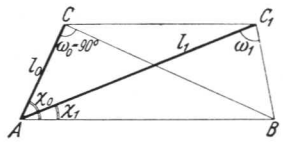

FIG. 46.—Origin of the Additional Markings.

From the triangles ABC and ABC_1 we obtain

$$\frac{l_1}{l_0} = d = \frac{\sin(\chi_1 + \omega_1)}{\cos \chi_0} \cdot \frac{1}{\sin \omega_1}$$

[1] These defects are, in general, found only on crystals drawn from the melt (Czochralski method).

Using the formula for the extension it follows that either

$$\operatorname{cotg} \omega_1 = \frac{\sin^2 \chi_0 - \sin^2 \chi_1}{2 \sin^2 \chi_1} \quad . \quad . \quad . \quad . \quad . \quad (29/1)$$

or

$$\operatorname{cotg} \omega_1 = \frac{d^2 \cos \chi_0 - \sqrt{d^2 - \sin^2 \chi_0}}{\sin \chi_0} \quad . \quad . \quad (29/1a)$$

These two formulæ give the angle between the plane of the groove and the longitudinal axis of the crystal as a function of the original position of the glide elements and their final position, or the amount of extension. It will be seen from formula (29/1) and from Fig. 46 that for values of χ_0 in excess of 45° the plane of the groove will come to lie once again perpendicularly to the longitudinal direction of the crystal, namely, when χ_1 (which is always $<\chi_0$) equals $(90° - \chi_0)$. Consequently in the initial positions $\chi_0 > 45°$ the traces of groove plane and glide ellipses coincide at the start of extension; whereas, however, in the course of further extension the glide ellipses remain inclined in the same direction, the plane of the grooves regains its upright position, reverts again to the transverse position, and then inclines in the opposite direction. If for the initial positions $\chi_0 < 45°$, then from the start of extension the plane of the groove, like the glide plane, approaches to the longitudinal axis but in the opposite direction.

B. MECHANICAL TWINNING

30. *Model of Twinning*

Viewed externally, mechanical twinning represents a type of plastic deformation entirely different from that of glide. It is a process by which portions of the stressed crystal discontinuously take up positions which are symmetrical to a plane or direction in the rest of the crystal. The symmetrical position of the two lattices in the undeformed and deformed parts is essential to this process, but not the symmetry of the external form. The latter occurs only when the crystal is bounded by certain crystallographic planes.

The best-known example of mechanical twinning is provided by the compression twins of calcite (Fig. 47). This type of deformation also occurs extensively with metal crystals (Fig. 48).

Macroscopically, deformation twins are formed by simple shear: plane layers glide by an amount proportional to their distance from the plane separating the undeformed from the deformed part, *i.e.*, the twinning plane. Fig. 49 illustrates this process by means of a wooden model.

The difference between twinning and glide appears clearly from Figs. 50 and 51. The illustrations show the lattice plane that passes

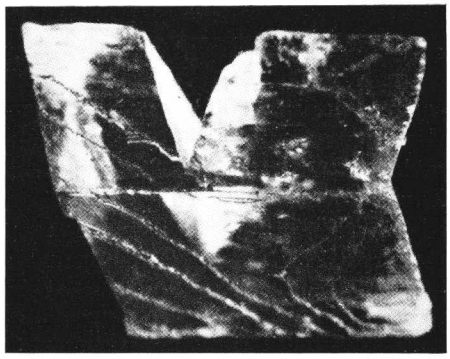

FIG. 47.—Calcite Twin, Produced by Insertion of a Knife (Baumhauer).

through the direction of shear and is perpendicular to the plane of shear. Whereas in glide the shear cannot amount to less than an

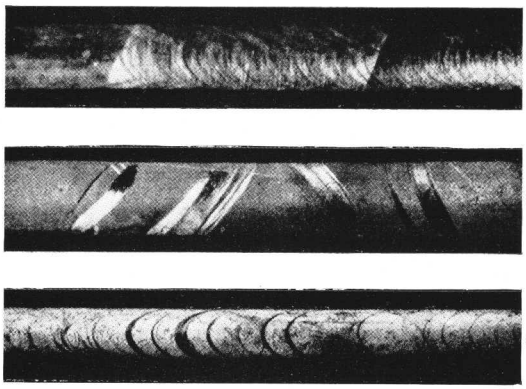

FIG. 48 (*a*)–(*c*).—Mechanical Twinning of Metal Crystals.

interatomic distance in the direction of glide (identity translation), the magnitude of displacement in twinning is usually no more than a small fraction of a lattice spacing. As is apparent from glide bands, the shear strain is by no means uniform over the whole length of the crystal in the case of glide. In mechanical twinning,

on the other hand, all planes in the deformed part which lie parallel to the shear plane are identically displaced with reference to the neighbouring plane. Consequently bands do not occur within a twin lamella. In the case of glide, the shear can take place in both

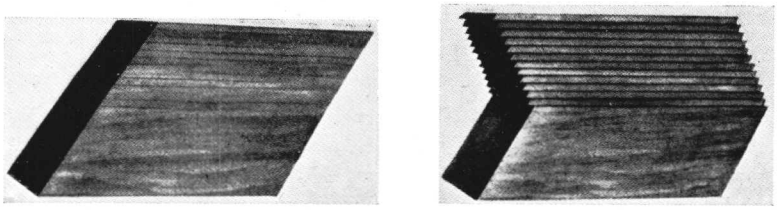

a *b*

FIG. 49.—Model of a Crystal (*a*) before and (*b*) after Simple Shear, showing the Mechanism of Twinning (According to Mügge).

directions (corresponding to the extension or compression of the crystal), whereas in twinning the shear direction is polar. This deformation process leads to a change in shape of definite type and

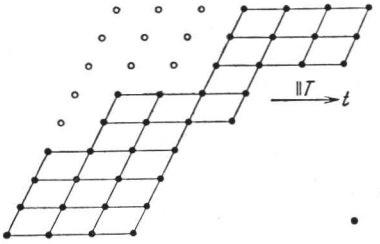

FIG. 50.

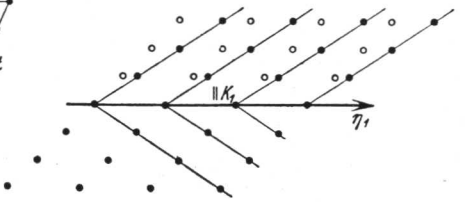

FIG. 51.

Movement of the Lattice Points in Glide and Mechanical Twinning (103).

magnitude, which is determined by the crystallographic nature of the twinning elements.

31. *Geometrical Treatment of Mechanical Twinning*

The geometrical relationships between the deformation occurring in twinning and the twinning elements will now be discussed with the aid of Fig. 52. The plane of the drawing is again the plane of displacement, and the perpendicular twinning plane (K_1) intersects it in the shear direction η_1. The intersection of the unit sphere with the plane of shear is also included in the form of a circle.

Twinning distorts the unit sphere into an ellipsoid of equal volume, and the intersection of this ellipsoid with the plane of shear is shown also. For the two extreme semi-axes of the ellipsoid, a and c, which lie in the plane of shear, the relationship $a \,.\, c = 1$ follows from the constancy of volume.

The shear plane (K_1) changes neither its shape (" 1st undistorted plane ") nor its position in the course of deformation. On the other hand, all other planes, together with the directions not contained in K_1, become tilted. One of the planes perpendicular to the plane of shear remains, similar to K_1, as a circle (" 2nd undistorted plane K_2"). η_2 represents the intersect of this plane on the shear plane. The amount by which a point at unit distance from the twinning plane is displaced is termed the shear strain s. It is related to the angle 2ϕ between the two undistorted planes. It follows from the triangle OAC and from the proportionality between gliding and the distance from $K_1 (AA_1 = s \,.\, OC)$ that

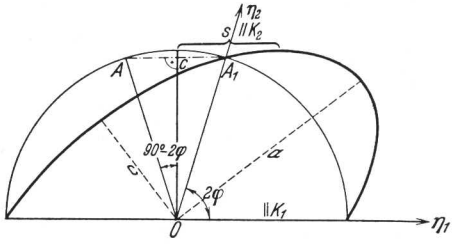

FIG. 52.—Diagram Illustrating the Geometrical Treatment of Mechanical Twinning.

$$tg 2\phi = \frac{2}{s} \quad . \quad . \quad . \quad . \quad . \quad . \quad (31/1)$$

The amount of shear is therefore fixed by the crystallographic nature of the two undistorted planes.

Since mechanical twinning is a simple shear, the resulting changes of length are again given by formula [(26/5) (108), (109)]. χ^* and λ^* now denote the angles between the longitudinal direction and the directions of K_1 and η_1, and the glide strain a should be replaced by the shear strain s. The formula for twinning is therefore :

$$\frac{l_1}{l_0} = d = \sqrt{1 + 2s \,.\, \sin \chi^* \cos \lambda^* + s^2 \,.\, \sin^2 \chi^*} \quad . \quad (31/2)$$

The condition $2s \sin \chi^* \times \cos \lambda^* + s^2 \sin^2 \chi^* = 0$ gives the geometrical position of the directions whose length remains unchanged in the course of twinning. For these directions we first obtain $\sin \chi^* = 0$, *i.e.*, the 1st undistorted plane. The second solution yields $-\dfrac{\sin \chi^*}{\cos \chi^*} = \dfrac{2}{s}$, or, employing equation (31/1) $-\dfrac{\sin \chi^*}{\cos \chi^*} = tg 2\phi$.

However, as can be easily ascertained from Fig. 53, this is the equation of the 2nd undistorted plane in its initial position.

With the aid of these two undistorted planes all the orientations on the pole sphere are divided into four regions, of which each opposite pair on twinning leads to either extension or compression. Extension occurs for all the directions contained in the obtuse angle between K_1 and the original position of K_2 (K°_2), and compression within those contained in the acute angle between the two planes (cf. also Fig. 52).

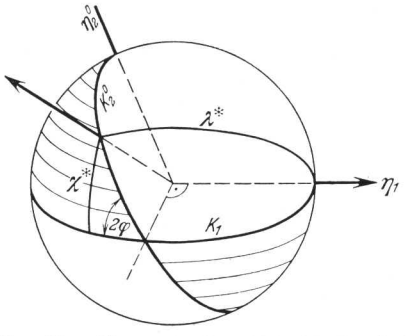

FIG. 53.—Change in Length in Mechanical Twinning: Extension in the Unshaded, Compression in the Shaded Portion.

Extreme values for changes in length are obtained for orientations in the plane of shear ($\chi^* = \lambda^*$), since outside this plane λ^* always exceeds χ^*. From the differentiation of the equation (31/2) in the case of $\chi^* = \lambda^*$, we obtain the orientation which leads to maximum extension or compression:

$$tg\chi^*_{1,2} = \frac{s}{2} \pm \sqrt{\frac{s^2}{4} + 1} \quad . \quad . \quad . \quad (31/3)$$

The amount of maximum extension or compression is obtained by inserting (31/3) in (31/2). For this purpose, equation (31/2) is transformed into

$$d = \frac{1}{\sqrt{1 + tg^2\chi^*}} \sqrt{1 + 2s \,.\, tg\chi^* + tg^2\chi^* + s^2 tg^2\chi^*}$$

It follows from (31/3) that $s \,.\, tg\chi^* = tg^2\chi^* - 1$ so that finally

$$d_{1,2} = \pm\, tg\chi^* \quad . \quad . \quad . \quad . \quad . \quad (31/4)$$

The choice of sign is fixed by the condition that $d = \frac{l_1}{l_0}$ must always remain positive.

The maximum extension is therefore

$$d_{\max.\ \text{extension}} = \frac{s}{2} + \sqrt{\frac{s^2}{4} + 1} \quad . \quad . \quad (31/4a)$$

and the maximum compression

$$d_{\max.\ \text{compression}} = -\frac{s}{2} + \sqrt{\frac{s^2}{4} + 1} \quad . \quad . \quad (31/4b)$$

For $l_0 = 1$ these two values represent the axes a and c of the deformation ellipsoid. Their product is unity, as is required by the constancy of volume.

The above formulæ show that the values of the shear strain (s) are small, and in contrast to glide the amount of deformation by twinning is therefore usually slight.

32. *Possibility of Twinning and Transformation of Indices*

Whereas a plane lattice represented by a net of parallelograms can always undergo twinning, this is not always so with space lattices. The condition which must be satisfied if mechanical twinning is to occur in a space lattice can be obtained from the following considerations [(110), (111)]. If, after twinning, each lattice point of the deformed portion is to have a corresponding point of the original lattice mirror reflected along the gliding surface (HKL), it should be possible before shear to join each pair of points in the lattice by lines which are parallel to the direction $\tau_{i2}[UVW]$ and which are halved by the glide plane. Let $[[mnp]]$ and $[[m_1n_1p_1]]$ be two points in a simple primitive space lattice, then the condition which must be fulfilled if their connecting line is to run parallel to $[UVW]$ is :

$$(m_1 - m) : (n_1 - n) : (p_2 - p) = U : V : W.$$

In addition the equation

$$Hm_1 + Kn_1 + Lp_1 = -(Hm + Kn + Lp)$$

indicates that the points on different sides are at the same distance from K_1. The solution of both equations according to m, n, and p leads to

$$m = m_1 - 2U\frac{Hm_1 + Kn_1 + Lp_1}{HU + KV + LW}$$

and two analogous equations for n and p.

Since mnp and $m_1n_1p_1$ must, according to definition, be whole numbers, while UVW as indices of a direction have no common factor, the denominator $HU + KV + LW$ must be either ± 1 or ± 2. Therefore this relationship between the indices of the shear plane and the direction τ_{i2} furnishes the condition for the possibility of twinning in a simple primitive lattice; it must be correspondingly modified for multiple centred lattices (111).

In conclusion, the following particulars are given of the transformation of indices for directions and planes which occurs with

mechanical twinning (112). Let $[UVW]$ and (HKL) be the indices of η_2 and K_1 or η_1 and K_2; then, if ϱ is a factor of proportionality the following transformation formulæ apply :

The direction $[uvw]$ is transformed into $[u'v'w']$ by

$$\left.\begin{aligned} \varrho u' &= u - 2U\,\frac{Hu + Kv + Lw}{HU + KV + LW} \\ \varrho v' &= v - 2V\,\frac{Hu + Kv + Lw}{HU + KV + LW} \\ \varrho w' &= w - 2W\,\frac{Hu + Kv + Lw}{HU + KV + LW} \end{aligned}\right\} \quad . \quad . \quad (32/2)$$

The plane (hkl) is transformed into $(h'k'l')$ by

$$\left.\begin{aligned} \varrho h' &= h(UH + VK + WL) - 2H(Uh + Vk + Wl) \\ \varrho k' &= k(UH + VK + WL) - 2K(Uh + Vk + Wl) \\ \varrho l' &= l(UH + VK + WL) - 2L(Uh + Vk + Wl) \end{aligned}\right\} \quad . \quad (32/3)$$

From these equations it will be apparent that, generally speaking, directions and planes change their indices consequent upon twinning. The indices remain unaltered for those directions which lie in the twin plane ($Hu + Kv + Lw = 0$) and for those planes which belong to the zone of η_2 ($Uh + Vk + Wl = 0$). In shear of type 2 (cf. Section 33) the directions in K_2 and the planes of the zone of η_1 retain their indices.

33. *Empirical Crystallographic Rules*

Hitherto we have discussed the model and the geometry of mechanical twinning. We will now examine briefly the crystallographic aspects of mechanical twinning and empirical data concerning observed twinning elements.

Glide plane K_1 or glide direction η_1 (or both together in cases of higher symmetry) are simple, rational lattice elements. Polyhedra with rational faces are also bounded after twinning by planes with rational indices.

If K_1 is rational, it is customary to speak of twinning of type 1. The deformed part of the crystal is the reflexion of the undeformed part with respect to the twinning plane. In this case we find that not only K_1 but also η_2, which is the intersection of the second undistorted plane with the plane of twinning, is also a rational lattice element. K_1 and η_2 serve to characterize twinning crystallographically. They define the plane of twinning, the direction of shear, the magnitude of shear and the second undistorted plane.

If η_1 is rational, the twinning is said to be of type 2. The deformed part of the crystal, compared with the original crystal, has now rotated 180° relative to the direction of shear. In this case K_2 is rational as well as η_1. Consequently both these elements are used to characterize a twinning of type 2, which in any case is observed only with crystals of low symmetry. The other elements of shear are then determined in the same way as described above.

The choice of twinning elements is also restricted in so far as K_1 cannot be a symmetry plane in twinning of type 1 (neither can it be perpendicular to an even-numbered axis of rotational symmetry); while in shear of type 2, η_1 cannot be a digonal axis, since it is only as a result of twinning that this lattice element acquires the character of a symmetry element.

CHAPTER VI

PLASTICITY AND STRENGTH OF METAL CRYSTALS

Chapter V contained a description of the general principles governing the change in shape of crystals during plastic deformation, together with the resultant changes in orientation. Both mechanisms of deformation—gliding and mechanical twinning—were discussed. We now turn to the technique and the results of experiments on the plastic deformation of crystals; for the present, we shall confine ourselves to crystals which, owing to their extreme ductility, provide excellent experimental material. The result of investigations on the plasticity and strength of salt crystals will be given in the next chapter.

A. ELEMENTS OF GLIDING AND TWINNING

34. *Determination of the Elements of Gliding*

The elements used in the characterization of gliding—the glide plane (T) and the glide direction (t)—can be determined in various ways.

It is not proposed to discuss here the goniometric and microscopic methods applicable to polyhedrons with plane faces. Instead, a description will be given of the new methods developed for opaque crystals which are not bounded by plane faces. These methods can be considered under several headings according to the conditions governing the experiment. When applying them, however, certain modifications or combinations are often necessary.

To take the simplest case first, let us consider a crystalline material which admits of substantial plastic extension, accompanied by the appearance of glide bands or striations indicative of the operation of a single glide system (cf. Fig. 35). In this case the glide plane (T) can often be found by means of a Laue photograph (with the incident beam perpendicular to the plane of the striation). If the glide plane is perpendicular to a symmetry axis of the crystal, the resulting symmetry of the Laue photograph will usually suffice to index the glide plane (Fig. 54). T is more difficult to determine when its normal does not coincide with a symmetry axis, since an exact evaluation of the Laue photographs is often greatly hampered by the pronounced asterism caused by previous extension (cf. Section 59).

In crystals which have been substantially stretched, the direction of slip (t) can be usually determined by means of a rotation photo-

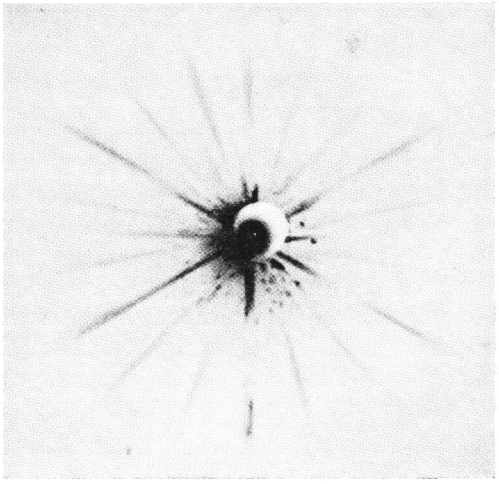

(*a*) Zn crystal: 6-fold picture: $T = (0001)$; (113).

(*b*) Al crystal extended at elevated temperature; 4-fold picture: $T = (001)$; (117).

FIG. 54 (*a*) and (*b*).—Determination of the Glide Plane (T) from the Symmetry of the Laue Photographs.

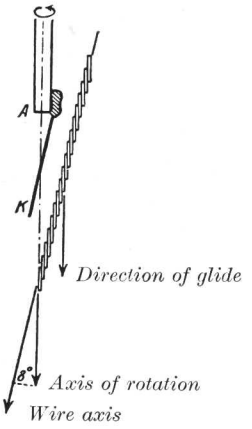

FIG. 55.—Adjustment of the Crystal in Order to Determine the Direction of Glide from Rotation Photographs.

graph (132). The position of t is indicated approximately by the intersection of T with the symmetry plane of the crystal band which is normal to the plane of the band and which contains its longi-

tudinal axis. Consequently the crystal is adjusted for the rotating-crystal photograph so as to ensure that the intersection of the glide plane with the median plane of the band to which reference has

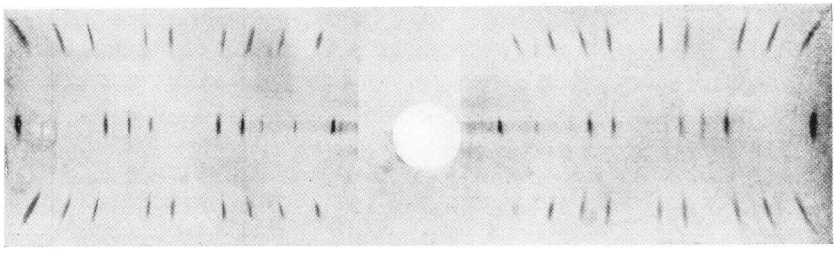

(*a*) Sn crystal; $t = [001]$; (114).

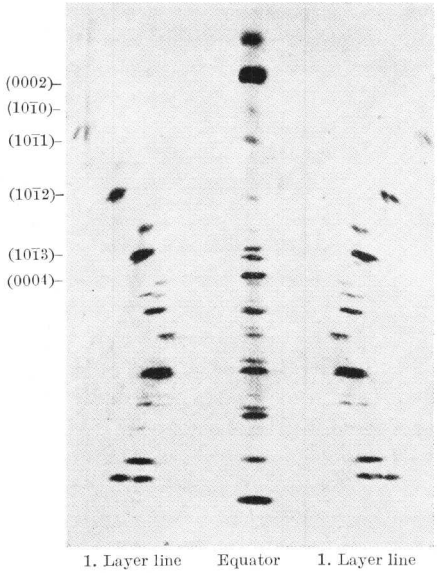

(*b*) Cd crystal; film axis = incidental beam; $t = [11\bar{2}0]$; (131).

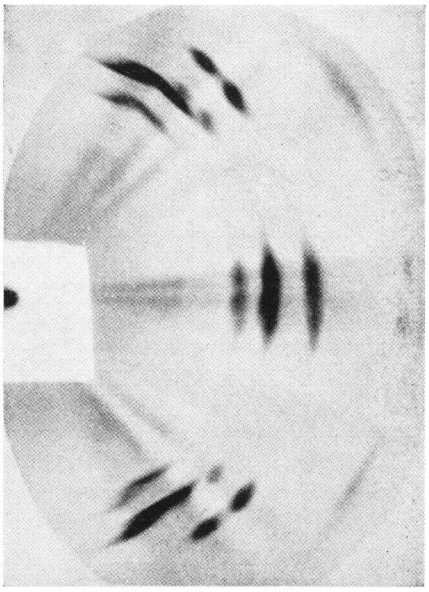

(*c*) Al crystal; extended hot; $t = [110]$; (117).

FIG. 56 (*a*)–(*c*).—Determination of the Direction of Glide (t) from Rotation Photographs.

already been made, forms the axis of rotation (Fig. 55). Thus the crystal wire describes a cone round the direction of glide, with a cone angle that corresponds to the small angle of inclination between T and the wire axis. Fig. 56 contains a few rotation photographs

which have been obtained in this way, and which, evaluated by means of the Polanyi layer-line relationship (formula 21/2), plainly reveal the crystallographic nature of the glide direction.

So much for the X-ray method, which supplies direct evidence of the elements of glide. We shall now consider a more indirect method for the determination of the glide *direction*. In this connection reference will be made to the change in orientation caused by glide during extension, which was discussed in Section 26. The change was found to be a movement of the longitudinal axis of the crystal towards the operative direction of glide. Consequently the method of obtaining t consists in determining that direction to which the longitudinal axis approaches as extension increases—having first ascertained the crystal orientation at various stages of extension. The resultant direction of glide can be checked by applying the formula for extension (26/1), which relates the amount of extension to the change of the angle between the longitudinal axis and the direction of glide. Fig. 57 shows the application of this method to a magnesium crystal which has been extended at elevated temperature. A digonal axis of type 1 was found to be the effective glide direction both for the initial glide in the direction of the basal plane and for the subsequent glide in the direction of a pyramidal plane.

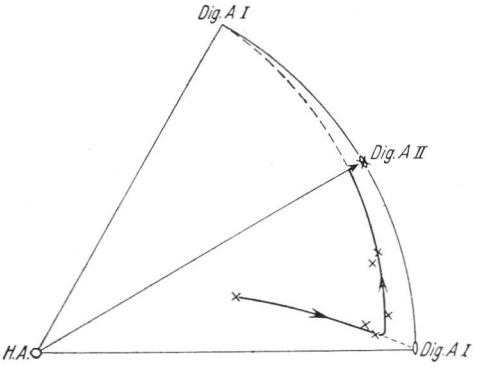

FIG. 57.—Determination of the Direction of Glide from the Lattice Rotation in the Course of Extension; Mg Crystal at >225° C. [see (129)].

Similarly, it is possible to determine the glide *plane* from the lattice rotation during compression, since in this case the change of orientation consists in a movement of the longitudinal direction towards the normal of the glide plane (checking the compressive strain by the formula 26/7). Tensile tests afford no direct indication of T apart from the fact that T contains the glide direction and must therefore belong to the zone of t. If, however, we make the obvious physical assumption that, where glide systems are crystallographically equivalent, that system will operate in which the resolved shear

stress is a maximum [1] it will be seen that in certain circumstances the glide planes can be determined from study of the lattice rotation alone. With the further assumption that the glide plane will have low indices, the whole range of orientations can be subdivided in such a way that the shear stress within each division is greater in one glide system than in the remaining crystallographically equivalent systems. If, on this assumption, the glide system which invariably operates is that in which the shear stress is a maximum, then the lattice rotation which accompanies extension in each division, and consequently in the total range of orientation, is established. A comparison of the experimentally ascertained lattice rotation with the changes of orientation which have been calculated on various assumptions about T, may serve to determine the glide plane.

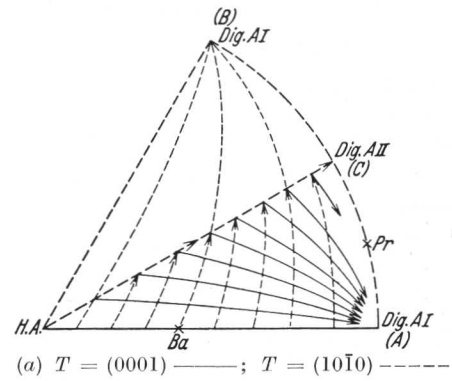

(*a*) $T = (0001)$ ———; $T = (10\bar{1}0)$ – – – –

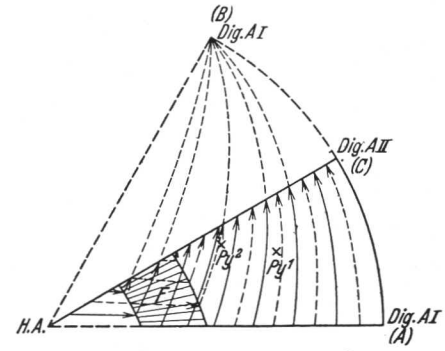

(*b*) $T = (10\bar{1}1)$ ———; $T = (10\bar{1}2)$ – – – –

FIG. 58 (*a*) and (*b*).—Indirect Determination of the Glide Elements of Hexagonal Crystals from the Lattice Rotation in the Course of Extension.

An example of the application of this method is shown in Fig. 58, in which the lattice rotation for the extension of close-packed hexagonal crystals is given $\left(\frac{c}{a} = 2\sqrt{\frac{2}{3}} = 1{\cdot}633\right)$. The diagram is based on a direction of glide parallel to the digonal axis, type I, and on glide planes parallel to the basal plane (0001), prism type I $(10\bar{1}0)$, pyramidal plane I, types 1 and 2 $(10\bar{1}1)$ and $(10\bar{1}2)$. Basal glide can be readily distinguished from the other three types by the fact that in the whole of the orientation triangle the wire axis moves

[1] It will be shown in Section 40 that this assumption is entirely justified.

towards the digonal axis type 1 (A) in a corner of the triangle (Fig. 58a). On the other hand, if one of the other three glide planes becomes operative the wire axis tends towards a digonal axis type 1 (B) lying outside the triangle for most initial orientations. With prism glide this occurs in the whole of the orientation triangle, whereas with pyramidal glide (Fig. 58b), sections adjacent to the hexagonal axis involve an initial rotation towards (A). By examination of the behaviour of crystals in the area F it is possible to distinguish between the two pyramidal glide planes. Whereas with basal glide a considerable degree of extension will result in an approach to a digonal axis type I (A) in the final stage, with prism and pyramidal glide a digonal axis type II (C) represents the final orientation of the longitudinal axis of extended crystals. It is achieved in this case by double glide on two equivalent systems.

In Section 40 we shall indicate a further possible method for determining the glide plane, by examining the dependence of the yield point upon orientation. The points which refer to this are shown in Fig. 58 as Ba, Pr, Py^1 and Py^2, which indicate the initial orientation for minimum values of the yield point.

G. I. Taylor and his associates in their investigations of the plastic deformation of metal crystals (116) adopted a method entirely different from that described above.

In this method it is not assumed that deformation is due to crystallographic glide; instead, the mechanism of deformation is deduced from changes in the shape of the test piece, or of the systems of lines drawn upon it. This can be illustrated by a compression test carried out on a cylindrical disc (115).[1] Two groups of lines are scratched on the compression surface of the plate, and their distortion under compression is observed. The axes of co-ordinates are such that the x-axis runs parallel to the lines, the y-axis passes at right angles to them through the compression surface, while the z-axis lies normal to the compression surface (parallel to the direction of compression). Let the co-ordinates of a given portion before and after deformation be $(x_0y_0z_0)$ and $(x_1y_1z_1)$. The transformation equations will then be [2]

$$\begin{aligned} x_1 &= \alpha x_0 + l y_0 + \mu z_0 \\ y_1 &= m y_0 + \nu z_0 \\ z_1 &= \gamma z_0 \end{aligned}$$

[1] Application of this principle to the tensile test is discussed in (121).

[2] Owing to the particular choice of the direction x, y_1 is independent of x_0. Planes parallel to the compression surface preserve this parallel position; consequently z_1 depends only on z_0 and the degree of compression.

α, l, μ, m, ν and γ are constants which can be calculated from the change in shape of the test piece and the distortion of the lines.

It is now necessary to establish the geometrical locus of all those directions which have not altered their length during deformation. This is governed by $x_0^2 + y_0^2 + z_0^2 = x_1^2 + y_1^2 + z_1^2$.

Adoption of the above transformation formulæ gives the equation of the "unstretched cone" in the initial position (cone-surface type 2). After introducing polar co-ordinates (θ = the angle between the observed direction and the z-axis, ϕ = the angle between the projection of this direction on the xy-plane and the x-axis), the equation of the unstretched cone surface is obtained in the form of $f(\theta, \phi) = 0$. With the help of this formula the θ values appropriate to the individual ϕ values can be calculated, and the unstretched cone surface expressed in a stereographic projection by using the xy-plane as projection plane. It is usually found that the unstretched cone surface has degenerated into two planes and that the deformation is therefore a plane one.[1]

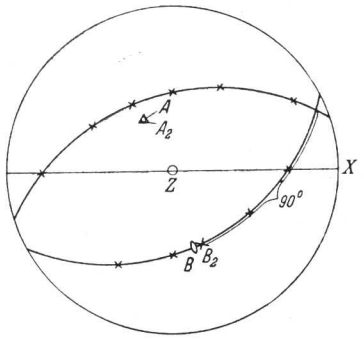

FIG. 59.—Stereographic Representation of the Unstretched Cone Surface of a Compressed Al Crystal (115).

Which of the two planes is the glide *plane* (T) can be determined in various ways. 1. A determination of the orientation of the crystal lattice with respect to the two planes before and after deformation reveals that only one of them (the one corresponding to T) retains its orientation relative to the crystal axes. 2. If glide bands occur during deformation these will usually suffice, even if only indistinct, to distinguish between the two planes. 3. The initial state and *two* stages of deformation are examined. The planes that remain undeformed are determined after the first and second deformation. One of them (T) will have retained its crystallographic character.

The *direction* of glide (t) is shown by this method to be that direction which is perpendicular to the intersection of the two planes in T (cf. the analogous geometrical discussion in Section 31 of the two undistorted planes in mechanical twinning).

As an example of the use of this method, Fig. 59 shows a stereo-

[1] If x_0, y_0 and z_0 are eliminated from the above condition, in place of x_1, y_1 and z_1, then we obtain the equation of the unstretched cone surface after deformation.

graphic projection of the unstretched cone surface of a compressed aluminium crystal, which clearly reveals degeneration into two planes. One of them corresponds to a (111) plane of the crystal, as will be seen from the coincidence of its normal (A_2) with a [111] direction (A). The direction (B_2) contained in this plane, and separated by 90° from the intersection of the two planes, very nearly coincides with a [101] direction (B). Consequently these two lattice elements, the octahedral plane (111) and the plane diagonal [10$\bar{1}$], have been recognized as the glide elements of the aluminium crystal.

By means of the unstretched-cone method it is also possible to analyse that type of crystal deformation (already discussed in Section 28) in which the two glide systems are equally favourably placed in relation to the direction of applied stress, although in this case the cone surface normally will not have degenerated into two planes. It is found that the deformation takes the form of double glide along the two equally favoured glide systems.

35. *The Glide Elements of Metal Crystals*

The results of existing determinations of the glide elements of metal crystals are given in Table VI. The last column contains the cleavage or rupture planes which have been observed in the crystals.

With cubic face-centred metals only octahedral glide occurs at room temperature. The position with regard to cubic body-centred metals is not yet clear. In the case of α-iron in particular, the existence of a " pencil "-glide in which only the *direction* of glide is supposed to be crystallographically fixed (121) [1] has been indicated. However, later work [(122), (123)] makes it seem highly probable that in this case too the selection of *both* glide elements proceeds strictly along crystallographic lines. In *hexagonal* metals the basal plane has hitherto always been found to be a unique glide plane with the three digonal axes type I as glide directions.

In the case of the tetragonal β-tin crystal, crystallographically non-equivalent glide systems are already found at room temperature. However, glide $T = (110)$, $t = [001]$ is greatly preferred. Among the rhombohedral metals only bismuth exhibits extensive glide. The best glide plane in this case is the basal plane, although the three equivalent (11$\bar{1}$)-planes appear also to occur as glide planes. It is not yet known for certain whether, in addition to the [10$\bar{1}$] directions, the [101] directions are also possible glide directions. The

[1] This mechanism is said to apply, within a certain range of orientation, to cubic body-centred β-brass also. The other orientations give glide with $T = (101)$, $t = [11\bar{1}]$ (125).

TABLE VI

Glide Elements and Cleavage Planes of Metal Crystals

Metal.	Lattice type, crystal class.	Glide elements. At 20°. $T.$	Glide elements. At 20°. $t.$	Glide elements. Additional at elevated temp. $T.$	Glide elements. Additional at elevated temp. $t.$	Close packed. Lattice planes.	Close packed. Lattice directions.	Literature.	Cleavage planes.
Aluminium .	Cubic face-centred O_h	(111)	[10$\bar{1}$]	from 450° C. (100)	[011]	1. (111)	1. [10$\bar{1}$]	(116), (117)	—
Copper .				—	—	2. (100)	2. [100]	(118), (119)	—
Silver .				—	—	3. (110)	3. [112]		
Gold .				—	—	—	—		
Lead .		(111)	—	—	—	—	—	(120)	—
α-Iron .	Cubic body-centred O_h	—	[111]	—	—	1. (101)	1. [111]	(121)	(001)
		(101)	[11$\bar{1}$]	—	—	2. (100)	2. [100]	(122)	—
		(112)							
		(123)							
		(123)	[11$\bar{1}$]	—	—	3. (111)	3. [110]	(123), (124)	—
Tungsten .		(112)	[11$\bar{1}$]	—	—	—	—	(126)	(001)
Magnesium .	Hexagonal close packed D_{6h}	(0001)	[11$\bar{2}$0]	from 225° C. (10$\bar{1}$1) or (10$\bar{1}$2)	[11$\bar{2}$0]	(0001)	[11$\bar{2}$0]	(127), (128), (129)	(0001), (10$\bar{1}$1), (10$\bar{1}$2), (10$\bar{1}$0)
Zinc .				—	—	—	—	—	—
Cadmium .				—	—	—	—	(130)	(0001)
				—	—	—	—	(131)	—
β-Tin (white)	Tetragonal D_{4h}	(110)	[001]	from 150° C. (110)	[$\bar{1}$11]	1. (100)	1. [001]	(132), (133)	—
		(100)	[001]	—	—	2. (110)	2. [111]	—	—
		(101)	[10$\bar{1}$]	—	—	3. (101)	3. [100]	—	—
		(121)				—	4. [101]	—	—
Arsenic .	Rhombohedral D_{3d}	—	—	—	—	1. (1$\bar{1}$0)	1. [$\bar{1}$01]	—	(111), 110)
Antimony .		—	—	—	—	2. (11$\bar{1}$)	2. [101]	—	(111), (110), (11$\bar{1}$)
Bismuth .		(111)	[10$\bar{1}$]	—	—	—	—	(134)	(111), (11$\bar{1}$), (110)
		(11$\bar{1}$)	also [101]	—	—	—	—	(135)	—
Tellurium .	Hexagonal D_3	(10$\bar{1}$0)	[11$\bar{2}$0] ?	—	—	(1011)	—	(136)	(10$\bar{1}$0)

plasticity of tellurium crystals merely takes the form of a slight flexibility, due to glide along the $(11\bar{2})$ plane, which is also a cleavage plane (prism plane type I in the hexagonal representation).

A study of Table VI reveals a clear connection between capacity for glide and density of packing—a connection which has long been recognized (137). It is invariably the most dense atomic row that serves as a direction of glide, and usually the planes of highest atomic density are the glide planes. Attempts to explain the glide elements in terms of lattice theory have so far been unsuccessful: considerations of glide in a packing of spheres with cubic face-centred and cubic body-centred symmetry threw no light on the glide elements which had been observed in these crystals (138); determination of the modulus of shear of various planes revealed that the operative glide elements are by no means characterized by a minimum value (139).

In no case did an increase in the temperature of the test lead to a disappearance of the glide elements which are operative at room temperature; on the contrary, in many cases new glide systems appeared. It is quite likely that a detailed investigation of plastic deformation at temperatures near the melting point would reveal new glide systems in many other cases.

Although most of the glide elements of metal crystals have been determined from static tensile tests, it should be specially noted that with all other types of stressing as well [compression, torsion, dynamic and alternating stressing, cf. (140)] the same glide elements, arising from the nature of the lattice, become effective.

In conclusion, it should be mentioned that the glide elements observed in the crystals of pure metals are always observed in the α solid solutions of the respective metals.

36. *Manifestations of Glide*

Having enumerated the glide elements observed in metal crystals we will now describe the occurrence of these elements under different types of stress, and the resulting lattice rotations.

The lattice rotation which occurs in an extended crystal where a single glide plane is present (hexagonal metals) is shown in Fig. 58*a*. If the initial orientation is near a prism plane of type II, a second and only slightly less favourable digonal axis type I becomes operative as a glide direction in the initial stages, so that glides tarts along the same plane in two directions (see Section 28). If the longitudinal axis lies exactly in a prism plane type II, both glides

persist, and the longitudinal axis of the crystal approaches increasingly a digonal axis type II, to which the two operative directions of glide are symmetrical. On the other hand, where the two glide directions are not equally favourable, the one which is preferred geometrically soon predominates, and the subsequent change in orientation proceeds as shown in Fig. 58*a* (129). The change of orientation as a result of pyramidal glide which occurs with magnesium at high temperatures has already been discussed (Fig. 57). The surface bands on the crystal which result from the new glide and the

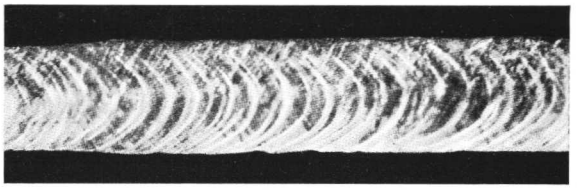

(*a*) In addition to the coarse markings resulting from basal glide, two additional systems of markings caused by pyramidal glide can be seen.

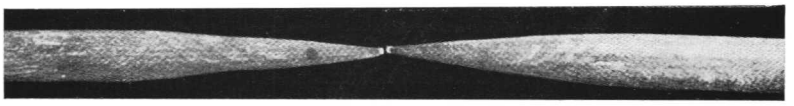

(*b*) Necking due to pyramidal glide.

FIG. 60 (*a*) and (*b*).—Mg Crystals Stretched at Elevated Temperatures (129).

change in the shape of the crystal (necking of the band) are shown in Fig. 60.

There are twelve equivalent glide systems available in the cubic face-centred metals (four octahedral planes, each with three face diagonals). The choice of system in the case of extension depends upon the direction of the tensile stress in relation to the crystallographic axes. As was explained at length for the case of aluminium (116), glide always occurs along the system subjected to maximum shear stress.[1] Fig. 61 indicates the choice of available glide systems for different directions of stress. Each triangle which, by the application of symmetry operations characteristic of the crystal, results in the whole of the orientation range being covered, is characterized by a definite most favourable glide system.

The lattice rotations which accompany plastic deformation in

[1] Calculation of the shear stress is dealt with in detail in Section 40.

extension can be illustrated by means of an experimental example [aluminium (Fig. 62)] and by Fig. 63 (which represents a section of

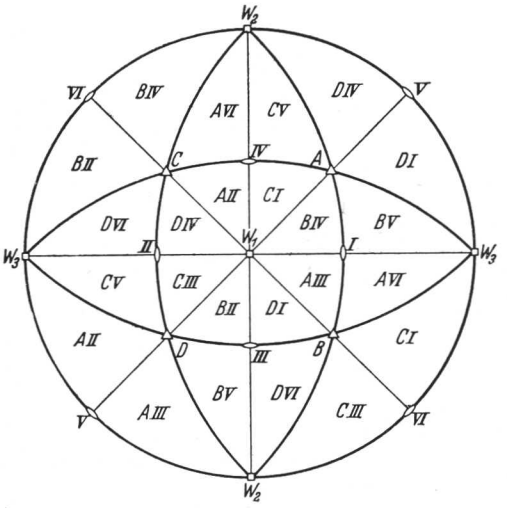

Fig. 61.—Choice of the Operative Octahedral Glide System for the Extension of Cubic Face-centred Crystals (116).

A–D : poles of the glide planes.

I–VI : glide directions.

Fig. 61). In the heavily outlined orientation area W_1AI, the most favourable glide system is B IV. Consequently, the lattice rotation

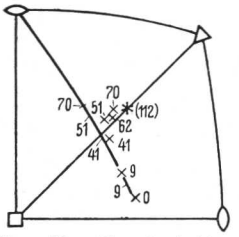

Fig. 62.—Reorientation during Extension of an Al Crystal (116).

× = orientation of the longitudinal axis after extension at the stated amount (%).

/ = orientations calculated on the assumption of simple glide.

[Formula (26/1).]

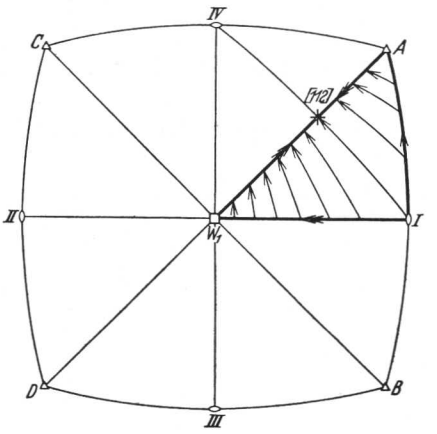

Fig. 63.—Lattice Rotation in the Course of Extension by Octahedral Glide.

which accompanies extension is indicated by the arrows pointing to IV. The glide direction IV, however, is not attained, for when the longitudinal axis enters the dodecahedral plane W_1A a second glide

system (CI) becomes geometrically equally favourable. The double glide along two systems which now sets in leads to a movement of the longitudinal axis in the symmetry plane W_1A towards the bisector [112] of the operative glide directions. The longitudinal

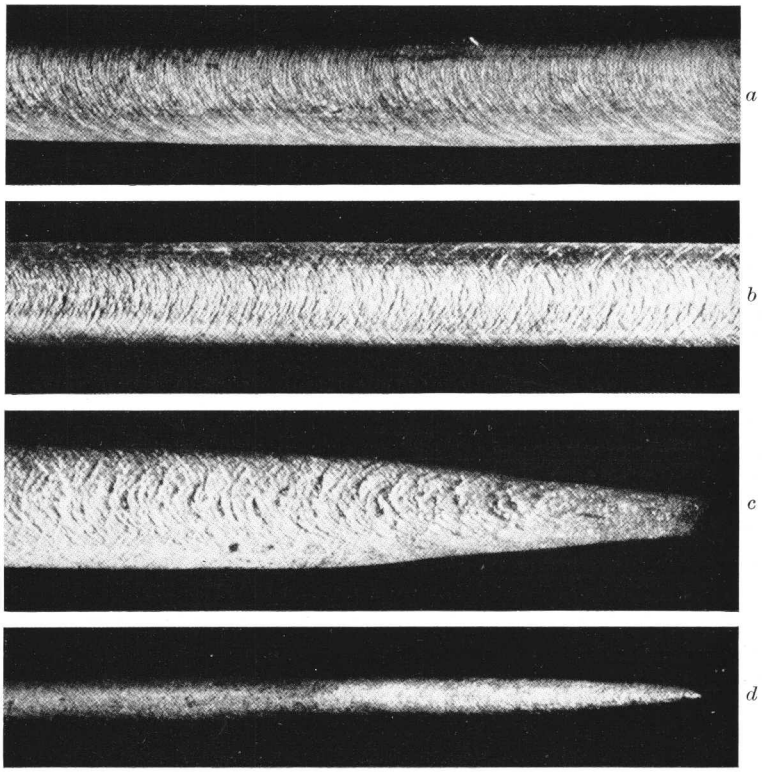

FIG. 64 (a)–(d).—Glide Bands on Al Crystals Extended at 400° C.
(a) and (b) simple and double octahedral glide. (c) and (d) cubic glide; viewed perpendicular and parallel to the plane of the original band.

axis of crystals extended at room temperature tends towards this direction.

Deviations from the normal case described above occur in the first place when the longitudinal axis of the crystals lies originally in a symmetry plane, so that from the outset two or more systems are equivalent [(141), (142)]. Secondly, deviations are observed at elevated temperatures. In this case, for initial orientations in the area AI [112] of the orientation triangle (Fig. 63), an aluminium

specimen, in addition to octahedral glide, will undergo cubic glide according to the most favourable system W_1V. Under the influence of these two glide systems the longitudinal axis tends towards a final position parallel to the body diagonal (A). The sequence of glide bands is shown in Fig. 64, a to d. Crystals in the orientation area W_1I [112] also exhibit irregular behaviour at elevated temperatures. In this instance several octahedral glides appear to become active even before the "symmetrals" are attained, thus resulting in a movement towards the cube edge W_1 [(117) cf. also (141) and (143)].

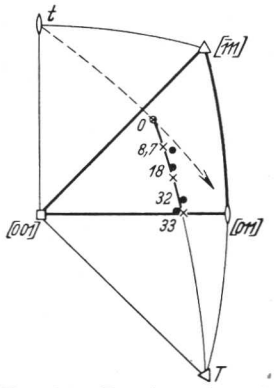

FIG. 65.—Reorientation of an Al Crystal as a Result of Compression (144).
● = as observed.
× = as calculated from formula (26/7) on the basis of the stated percentages of compression.

In the compression of aluminium crystals, too, that octahedral glide system in which the resolved shear stress is a maximum is the first to come into operation (144). The subdivision of the entire field of orientation into regions of equally favourable glide systems is the same as in the tensile test (Fig. 61), since it is only the sign of the stress that has changed. As already indicated in Section 26, however, the lattice rotation which accompanies the operation of an octahedral glide system is not that obtained by an inversion of the sign from the rotation in extension. It rather consists in a movement of the "longitudinal direction" towards the normal to the operative glide plane. This is illustrated in Fig. 65.

37. *Determination of Twinning Elements*

Like the glide elements, the twinning elements (twin plane K_1, and direction η_2 for twinning of type 1; 2nd undistorted plane K_2

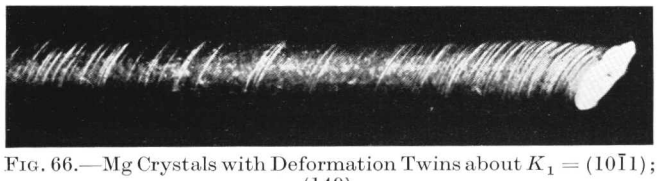

FIG. 66.—Mg Crystals with Deformation Twins about $K_1 = (10\bar{1}1)$; (149).

and shear direction η_1 for twinning of type 2) can be determined by various methods. In principle, the problem is solved when the

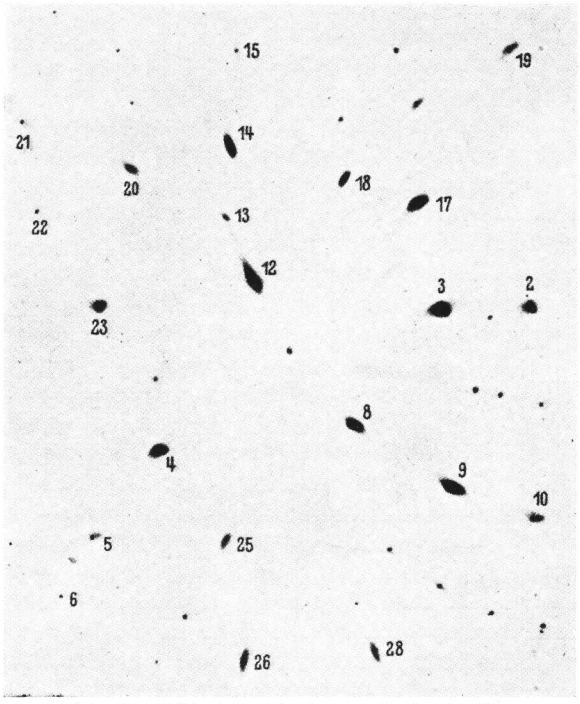

(*a*)—Laue Photograph Perpendicular to K_1.

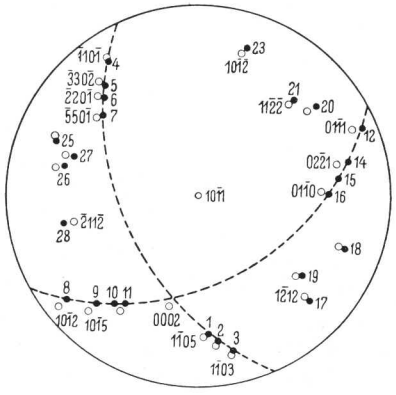

(*b*) Pole figure of the reflecting planes; close agreement with the pole figure about (10$\bar{1}$1).

Fig. 67 (*a*) and (*b*).—Determination of Twin Planes from Laue Photographs: Mg Crystal (149).

indices for several (at least two) crystallographic planes are known, both before and after twinning. With plane crystal boundaries they can be determined by a microscopic and goniometric measurement of the twin lamellæ. The transformation formulæ (32/3), resolved

with respect to (HKL) and $[UVW]$ then furnish the crystallographic indices of the twinning elements.[1]

However, in the case of the metal crystals with which we are mainly concerned there are as a rule no crystallographically bounded polyhedrons. We therefore propose to describe the methods to be applied in cases where the crystal "habit" is absent. These methods, however, only lead directly to the first undistorted plane K_1.

K_1 can be determined directly in all cases where a Laue photograph is obtainable at right angles to the twinning plane. For this it is necessary that the position of the plane should be adequately defined by twin bands. Figs. 66 and 67 illustrate the use of this method in establishing the $(10\bar{1}1)$ plane as the twinning plane of magnesium. Difficulties may arise owing to the pronounced distortion of the interference spots (asterism, see Section 59) which sometimes makes the evaluation of the diagrams impossible.

A second way of determining K_1 (or η_1) by X-rays is open in cases where it is possible to produce in the crystal a twin lamella so broad that not only the orientation of the initial crystal but also that of the twin can be determined, with respect to the same system of co-ordinates, by means of Laue photographs or photographs taken with an X-ray goniometer. The relative orientation of the two lattices is determined by the law of twinning: they arise from each other by reflexion on the twinning plane K_1 (or by rotation through 180° round the direction of glide η_1). If then the pole figures for the initial and the twinned positions are plotted in the same stereographic plot, it will be found that for twinning of the first type the position of *one* plane will be identical in both parts of the crystal, and this will correspond to K_1. Reflexion at its pole transforms corresponding directions into one another. In case of a twinning of the second type a rational crystal direction η_1 is common to both lattices which transform into each other by rotation through 180° round this direction. It is easier to find the twinning element in crystals containing unique sets of crystallographic planes; in such cases the twinning element bisects the angle between the two positions of the unique plane. Although this method has not so far led to the discovery of new twinning elements, it has in many cases confirmed previous results [(145), (146), 147)].

Another method which has been successfully used for determining K_1 involves measurement of the angles of twinning lamellæ with respect to a crystallographically known system of co-ordinates (148). On a specimen of very coarse-grained material or a single crystal, two

[1] This is conditional on the second plane not being also in the zone which is determined by the first plane when in the original and twinning position.

faces are ground inclined to each other at a known angle (in the simplest case they may be perpendicular to each other), and then by a slight compression twinning is produced in individual grains. After the surfaces have been polished again the angles between the twin and the reference planes can be measured, as well as those between the twin planes, should several sets of twins appear. It is a condition of this method that the same twin lamella must be recognizable on both polished surfaces (see Fig. 68). If the positions of the reference planes with respect to the crystallographic axes are known, the positions of the twin planes with reference to these axes can also be determined. If there are several sets of equivalent twin planes, their crystallographic nature is already revealed by the angles between them.

The three methods described above for boundaries which are not well-defined crystal planes, lead solely to the first undistorted plane K_1. The second of these methods is the only one that is capable of indicating, in addition, the direction of glide η_1 and thus also the plane of the shear. But with crystals characterized by a high degree of symmetry, as in the case of metals, the following consideration will lead to the determination of η_1 in the other methods also. If there is a symmetry plane at right angles to K_1, this plane must coincide with the plane of shear, and so its intersection with K_1 must be η_1. Otherwise the symmetry plane which was originally present would lose this property in the twinned portion. This is immediately obvious from the fact that in planes at right angles to the plane of shear only those directions which form equal angles with the plane of shear suffer equal distortion during twinning. If there were in addition a symmetry plane at right angles to K_1 and *inclined* towards the plane of the shear, directions symmetrical in relation to this plane would also suffer equal distortion, an assumption which cannot be reconciled with the mechanism of twinning.

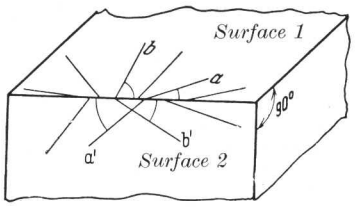

FIG. 68.—Determination of K_1 by Measuring the Traces of Twin Lamellæ on Two Polished Surfaces of the Crystal (148). Be Crystal.

If in addition to K_1 the indices of a direction or a plane are known before and after twinning, the indices $[UVW]$ of the direction η_2, together with the second undistorted plane and the shear strain, can be calculated from the equations (32/2) or (32/3).

In very elementary cases it should be possible, if K_1 and η_1 are known, to determine the second undistorted plane K_2 and η_2 by observing the movement of the lattice points in the plane of shear (cf. the following section).

38. *The Twinning Elements of Metal Crystals*

A summary of the elements of shear which have so far been observed in the mechanical twinning of metal crystals is given in Table VII. In addition to the two undistorted planes the amount

TABLE VII

Shear Elements of Metallic Crystals

Metal.	Lattice type, crystal class.	1st undistorted plane, K_1.	2nd undistorted plane, K_2.	Amount of shear, s.	Literature.
α-Iron	Cubic space centred O_h	(112)	$(11\bar{2})$	0·7071 $(= 1/2\sqrt{2})$	(150)
Beryllium	Hexagonal close packed D_{6h}	$(10\bar{1}2)$	$(10\bar{1}\bar{2})$ [1]	0·186	(148)
Magnesium		$(10\bar{1}2)$	$(10\bar{1}\bar{2})$ [1]	0·131	(148)
		$(10\bar{1}1)$			(151)
Zinc		$(10\bar{1}2)$	$(10\bar{1}\bar{2})$	0·143 $= \left(\frac{(c/a)^2 - 3}{c/a\sqrt{3}}\right)$ †	(148, (152)
Cadmium		$(10\bar{1}2)$	$(10\bar{1}\bar{2})$ *	0·175	(148)
β-Tin (white)	Tetragonal D_{4h}	(331)	$(11\bar{1})$	0·120	(153)
Arsenic	Rhombohedral D_{3d}	?(011)	(100)	0·256	(154)
Antimony		(011)	(100)	0·146	(155), (156)
Bismuth		(011)	(100)	0·118 $= \left(\frac{2\cos\alpha}{\sin\alpha/2}\right)$ ‡	(156)

* In these cases K_2 has not yet been determined. In line with the behaviour of the Zn crystal, $(10\bar{1}\bar{2})$ has been adopted as the 2nd reference circle and used for the calculation of s.

† c and a = lengths of axes.

‡ α = angle of the rhombohedron.

of the shear is also indicated. The table contains no particulars of the numerous instances of *recrystallization twins* in metals; these occur frequently during recrystallization after previous cold working.

The results of quantitative investigations on cubic metals are

available so far for body-centred α-iron only. Here the two undistorted planes are crystallographically equivalent, and so, too, are the direction of shear and η_2 ([111]-directions). When K_1 and K_2 or η_2 and η_1 can be interchanged, the shears are said to be reciprocal. If twinning occurs on several planes, internal cavities are formed : Rose's channels [(157), (158)]. These cause an increase in volume which may be substantial, and which in the case of iron may amount theoretically to as much as 50 per cent. (159). Although mechanical twinning has been repeatedly observed with cubic face-centred metals [see for instance (159*a*)] it has not yet formed the subject of systematic investigations. However, it is possible that in this case K_1 is identical with the twinning plane (111), which is always observed with recrystallization twins. This assumption points to $(1\bar{1}0)$ as a plane of twinning, to $\eta_1 = [11\bar{2}]$ and, in accordance with the movement of the lattice points in the plane of shear as shown in Fig. 69, to $K_2 = (11\bar{1})$, $\eta_2 = [112]$ and $s = 1/2\sqrt{2} = 0{\cdot}7071$ [1] [cf. (138)].

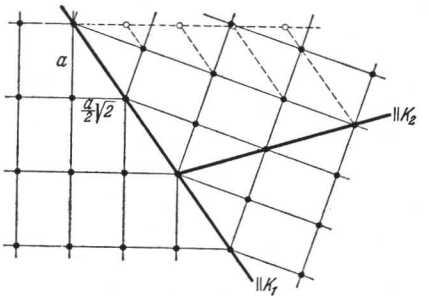

FIG. 69.—Simple Shear of Cubic Face-centred Crystals having $K_1 = (111)$ (Plane of Shear).

In the case of the hexagonal metals, twinning has hitherto been observed to occur on a pyramidal plane type I, order 2. Here we have a *single* glide plane in contrast to *six* planes of twinning. An exact determination of K_2 is available for the zinc crystal only, for which, apart from the direct determination of K_1, it was also possible to ascertain the indices of a plane (basal) before and after twinning. The particulars of K_2 and s in other cases have hitherto been inferred from analogy only. A consideration of the movements of the lattice points in the plane of displacement shows that in the case of the hexagonal metals, twinning is by no means a simple shear with the stated strain (s). Only a quarter of the lattice points are conveyed by this movement into the twin position. The remainder have still to carry out additional displacements towards or parallel to K_1 [(160), (152)]. With magnesium crystals in rare cases the pyramidal plane order 1 has been observed as a twinning plane, in

[1] These provisional shear elements of the cubic face-centred metal crystals fulfil the conditions of twinning for this type of lattice.

addition to the pyramidal plane of type 1, order 2. The *tetragonal* lattice of white tin is not capable of twinning with the elements mentioned above (161), so that here, too, the actual movement of the lattice points must differ substantially from a simple shear. Similarly the individual atoms of *rhombohedral* bismuth (and antimony) follow no straight line when twinning. On the other hand, the movement of the centres of gravity of pairs of co-ordinated atoms on the trigonal axis corresponds to simple shear (162).

Already this brief description confined to metal crystals shows how complicated are the circumstances in mechanical twinning — a fact which is abundantly confirmed by the numerous observations on salt crystals.

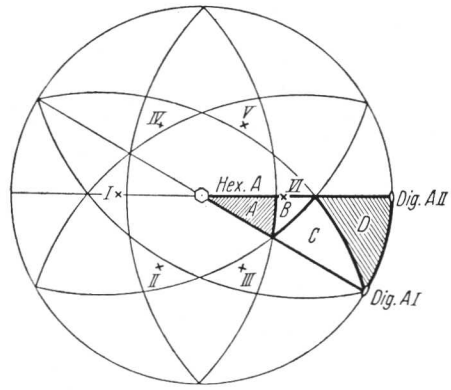

Fig. 70.—Change in Length as a Function of Orientation in the Case of Mechanical Twinning of Zn Crystals (163).

I–VI, poles of the twin planes.
A : I–VI, compression.
B : II, III, V and VI, compression; I and IV, extension.
C : II and V compression; I, III, IV and VI, extension.
D : I–VI, extension.

39. *Operation of Mechanical Twinning*

Now that particulars have been given of the elements of twinning observed with the various metals, we will proceed to a description of their operation under various types of loading.

First we must deal with the sign of the change in length due to twinning, since, owing to the polarity of the directions of glide, either only extension or only compression, according to the orientation, can occur in the direction considered (see Fig. 53). Fig. 70 represents a subdivision of the orientation field of the zinc crystal, based on its six twin planes $(10\bar{1}2)$. Directions at angles of between 0° and approximately 50° to the hexagonal axis are shortened by twinning on each of the six planes; while directions approximately at right angles to the hexagonal axis undergo extensions. A transition between the two is found in orientation regions in which some of the twinning planes produce extension and others compression. The same applies to cadmium crystals.

The change of shape is just the opposite for the important group of *hexagonal crystals* having an axial ratio c/a of approximately

Operative K_1 plane :

1, 2, 7, 8 : extension occurs in the whole of the orientation region.

3, 4 : compression in the whole of the region.

5, 11 : in EBC extension, in ABE compression.

6, 12 : in $EBDC$ extension, in ADE compression.

9, 10 : in BCD extension, in ACD compression.

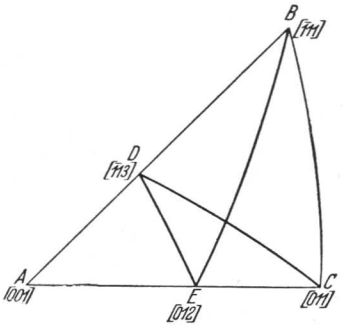

FIG. 71.—Mechanical Twinning of α-Fe. Orientation Regions in which Extension and Compression Occur. K_1 Planes Numbered 1–12 in Accordance with Fig. 11.

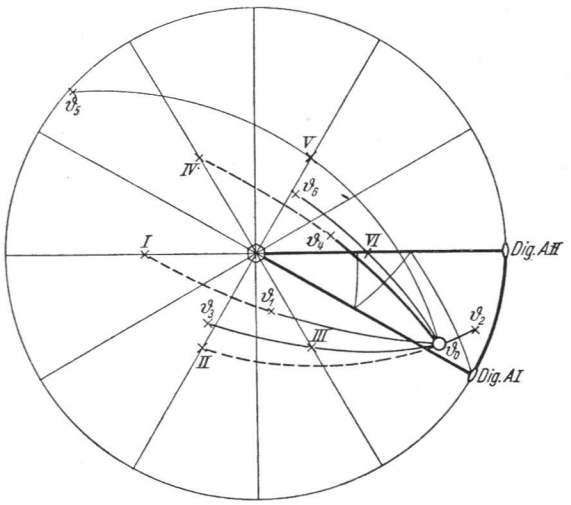

FIG. 72.—Change of Orientation with the Twinning of Zn.

(N.B.—In the text, $\vartheta = \theta$.)

1·63 (Mg, Be, etc.). In this case the hexagonal axis makes an angle of more than 45° with the twin planes (and, on the very probable

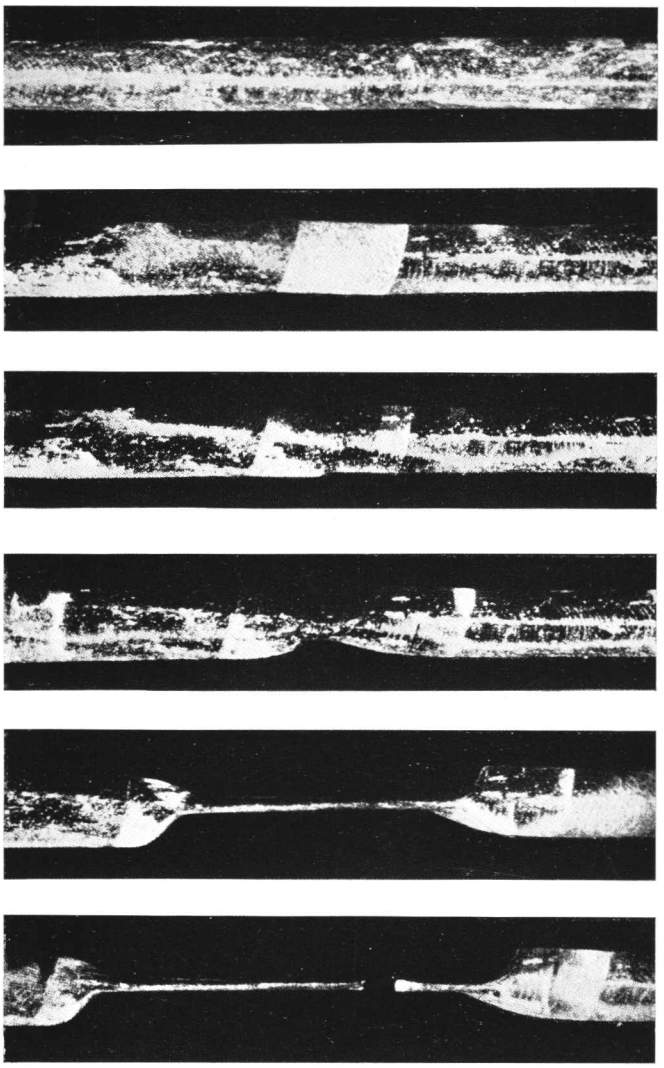

(*a*) Unetched crystal.

assumption of a reciprocal shear, also with the second undistorted planes), which means that the hexagonal axis and the adjacent

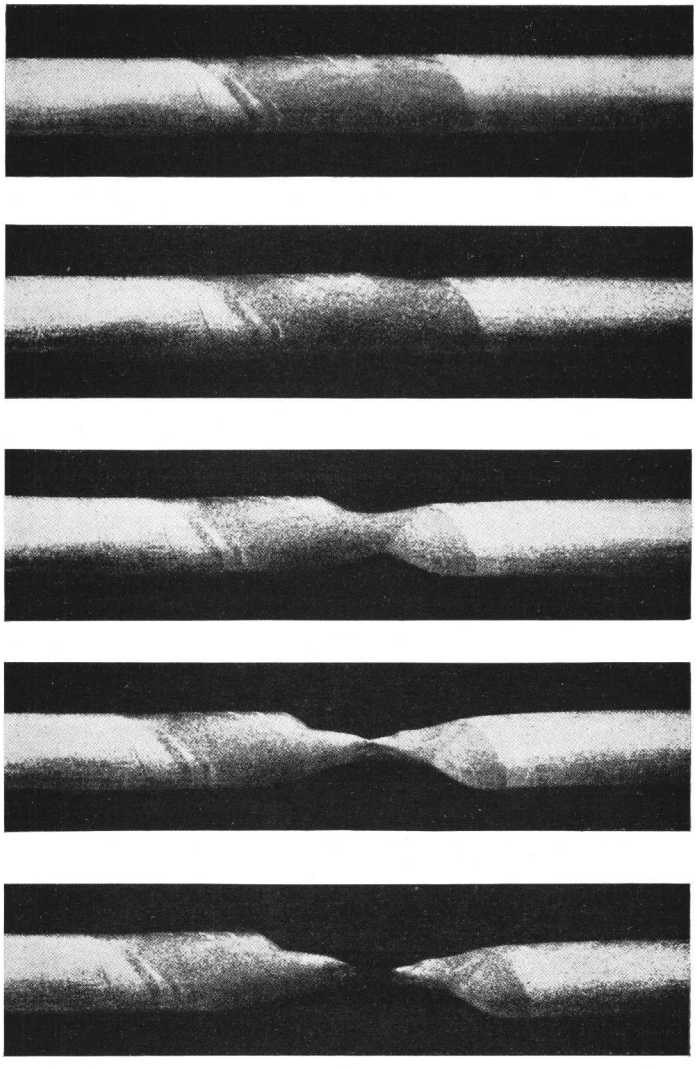

(*b*) Etched crystal.

FIG. 73 (*a*) and (*b*).—Secondary Basal Glide in the Twin Lamellæ of Zn Crystals. Viewed Perpendicularly to the Plane of the Band Resulting from Primary Basal Glide.

directions are *extended* by twinning on $(10\bar{1}2)$. As a rule, any twinning process that produces extension with zinc (and cadmium) leads to compression, and vice versa. Crystals with an axial ratio of $c/a = \sqrt{3}$ form the boundary between these two groups of crystals exhibiting opposite characteristics. Twinning on a $(10\bar{1}2)$ plane is impossible in this case, since the intersection of the plane of displacement with the hexagonal cell would represent a *square* of the length of the side $a\sqrt{3} = c$, with a diagonal in the direction of movement.

With body-centred α-iron having $K_1 = (112)$ and $K_2 = (11\bar{2})$ we obtain, for the twelve available twin planes, the subdivision of the basic triangle shown in Fig. 71. In this case there are no areas in which the formation of twins on all twin planes results exclusively in either extension or compression. The directions [012] and [113] are the corners of the resulting subdivisions.

Contrary to glide, mechanical twinning produces *no continuous change* of orientation; it transfers the lattice discontinuously into a new position. Fig. 72 illustrates this re-orientation, again for the case of the zinc (cadmium) crystal. The crystallographic system of co-ordinates is retained in this diagram. If the orientation of a given direction in the initial state is θ_0, then its position *after* twinning (θ_1 . . . . . θ_6) is obtained by reflexion on the six $(10\bar{1}2)$ planes. The choice of the initial position θ_0 results in a shortening of the direction considered in two of the twins (θ_2 and θ_5), and a lengthening in the other four.

Owing to the small extent of plastic deformation by twinning, its immediate importance for large-scale deformations of crystals is slight. Indirectly, however, and especially where hexagonal crystals are concerned, it can exert an important influence on plasticity. Owing to the characteristic swing-over of the lattice, a glide plane that is unfavourably situated to the direction of tension can suddenly adopt a position very favourable to further glide (*e.g.*, θ_1, θ_3, θ_4 and θ_6 in Fig. 72). Thus further appreciable increases of plastic deformation by glide, which otherwise would have been impossible, are facilitated by the conditions created by mechanical twinning. Zinc and cadmium crystals illustrate this very clearly [(148), (152)]. The " secondary extension ", a new glide which occurs after the principal extension by basal glide has become exhausted, represents a basal glide in a twin band in which, owing to the swing-over of the lattice through an angle of about 60° to the direction of tension, the basal plane has taken up a position highly favourable to further extension (see Fig. 73, *a* and *b*).